4
Aircraft Gas Turbine Engine

4.1 Introduction

The introductory fundamentals of aircraft propulsion systems are covered in this chapter. Emphasis is placed on propulsion systems that operate on the so-called Brayton cycle. Such systems include turbojets, turboprops, turbofans, ramjets, and combinations thereof. Before taking up the thermodynamic processes involved in these systems, we consider the forces acting on a propulsive duct and the effect of installation on the net propulsive force.

4.2 Thrust Equation

We define a *propulsion system* as a unit submerged in a fluid medium about and through which the fluid flows. The propulsion system contains an energy-transfer mechanism that increases the kinetic energy of the fluid passing through the system. This mechanism is called the *engine*. In Fig. 4.1, the engine is shown schematically in a nacelle housing that forms the second portion of the propulsion system. Thus the propulsion system contains:

1) An engine (the nozzle is considered to be part of the engine in our terminology),
2) Housing about the engine (nacelle or duct).

Several different aircraft systems may use the same engine submerged in different-shaped nacelles. Thus one propulsion system may use engine X in a pod installation hanging from a wing while, in another system, engine X may be surrounded by a nacelle that is, in fact, the airplane's fuselage—examples are the F-15 vs F-16 propulsion systems that use the F-100 turbofan engine. The thrust of a propulsion system will depend on 1) its engine and 2) its nacelle.

As a result, it is conventional to speak of *uninstalled engine thrust and installed engine thrust.* The uninstalled engine thrust should depend on the engine alone and hence must be independent of the nacelle. the installed engine thrust is the thrust produced by both the engine and the nacelle. Installed engine thrust T is defined as the shear force in the reaction strut of Fig. 4.1.

Uninstalled engine thrust F is defined as the force F_{int} acting on the internal surface of the propulsion system from 1 to 9 plus the force F'_{int} acting on the internal surface of the stream tube 0 to 1 that contains the air flowing into the engine. It will be shown that F is independent of the nacelle.

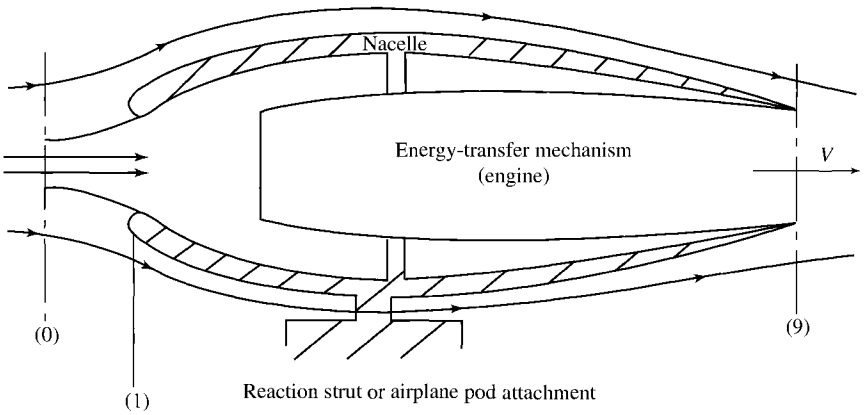

Fig. 4.1 Propulsion system.

To evaluate the uninstalled engine thrust, defined as $F_{\text{int}} + F'_{\text{int}}$, we apply the momentum equation to the control surface of Fig. 4.2. In so doing, we use the convention that all pressures used will be gauge pressures. We adopt this convention because it is used by the external aerodynamicist in computing the drag and lift forces on the airplane. To be consistent, then, the internal aerodynamicist must do the same. Figure 4.3 shows the momentum equation for assumed steady flow applied to flow through the control surface of Fig. 4.2.

Referring to Fig. 4.3 and equating forces to the change in momentum flux, we get

$$F'_{\text{int}} + F_{\text{int}} + (P_0 - P_0)A_0 - (P_9 - P_0)A_9 = \frac{\dot{m}_9 V_9 - \dot{m}_0 V_0}{g_c}$$

$$F + 0 - (P_9 - P_0)A_9 = \frac{\dot{m}_9 V_9 - \dot{m} V_0}{g_c}$$

$$\text{Uninstalled engine thrust} \quad F = \frac{\dot{m}_9 V_9 - \dot{m}_0 V_0}{g_c} + (P_9 - P_0)A_9 \tag{4.1}$$

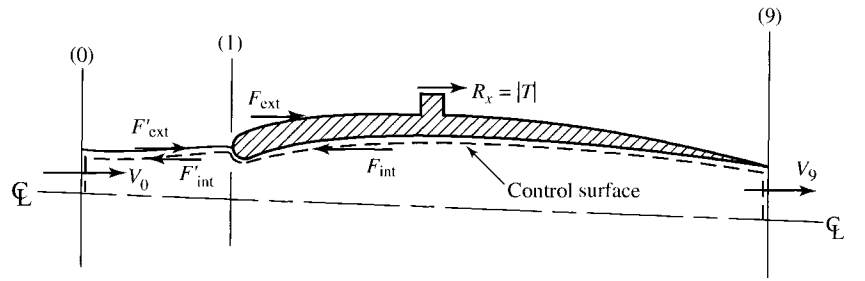

Fig. 4.2 Forces on propulsion system.

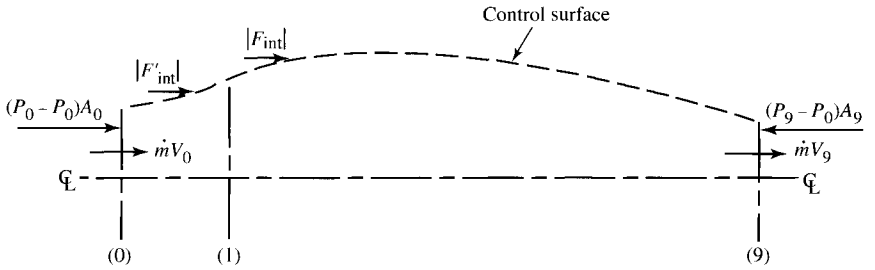

Fig. 4.3 Control surface forces and momentum fluxes for evaluating F (pressure referred to P_0).

This equation for the uninstalled engine thrust is seen to contain terms completely independent of the nacelle of the propulsion system. The terms $\dot{m}$, V_9, A_9, and P_9 are fixed by the engine while the terms V_0 and P_0 are fixed by the flight condition.

To obtain the installed engine thrust, we must "subtract" from the uninstalled engine thrust the drag forces F'_{ext} and F_{ext}. The first, F'_{ext}, is equal in magnitude to F'_{int} and adjusts the engine thrust for the force F'_{int}, which is credited to the uninstalled engine thrust but does not really contribute to the installed engine thrust. The second, F_{ext}, is the drag force acting on the external surface of the nacelle. Thus

F'_{ext} = pressure force on external stream tube surface from 0 to 1, which is called *additive drag* (Refs. 24, 25, and 26) or *preentry drag* (Ref. 27)

and

F_{ext} = pressure force on nacelle's external surface

In the accounting system of viscous and pressure forces acting on the airframe and engine, the viscous forces on the nacelle are included in the airframe drag, and the pressure forces on the nacelle are included in the installed engine thrust.

The installed engine thrust T is then

$$\text{Shear force in strut of Fig. 4.1} = T = F_{int} - F_{ext}$$
$$= F_{int} + F'_{int} - (F_{ext} + F'_{ext})$$

where $F_{int} + F'_{ext}$ is called the *drag* D and where, as in the preceding, $F_{int} + F'_{int}$ is called the *uninstalled engine thrust* F. Using this notation, we have

$$\text{Installed engine thrust } T = F - D \tag{4.2}$$

The two forces F_{ext} and F'_{ext} that make up the drag D are called the *nacelle drag* D_{nac} and the *additive drag* D_{add}, respectively. Thus the drag force can be written as

$$D = D_{nac} + D_{add} \tag{4.3}$$

In computing the pressure force in the drag term, we must reference all pressures to ambient pressure P_0. Thus the pressure drag on the external surface of the nacelle is

$$D_{nac} = \int_1^9 (P - P_0)\mathrm{d}A_y \tag{4.4}$$

where P is the absolute pressure on the nacelle surface $\mathrm{d}A$, which has a vertical component of $\mathrm{d}A_y$. The additive drag is the pressure drag on the stream tube bounding the internal flow between stations 0 and 1, or

$$D_{add} = \int_0^1 (P - P_0)\mathrm{d}A_y \tag{4.5}$$

Application of the momentum equation to the stream tube shown in Fig. 4.4 between stations 0 and 1 gives

Forces on stream tube = change in momentum flux

$$\int_0^1 (P - P_0)\mathrm{d}A_y - \int_1 (P - P_0)\mathrm{d}A_y = \int_1 \frac{\rho V^2}{g_c}\mathrm{d}A_y - \int_0 \frac{\rho V^2}{g_c}\mathrm{d}A_y$$

Thus

$$D_{add} = \int_1 \left(P + \frac{\rho V^2}{g_c}\right)\mathrm{d}A_y - \int_0 \frac{\rho V^2}{g_c}\mathrm{d}A_y - P_0 A_1$$

or

$$D_{add} = \int_1 \left(P + \frac{\rho V^2}{g_c}\right)\mathrm{d}A_y - \int_0 \left(P + \frac{\rho V^2}{g_c}\right)\mathrm{d}A_y - P_0(A_1 - A_0) \tag{4.6}$$

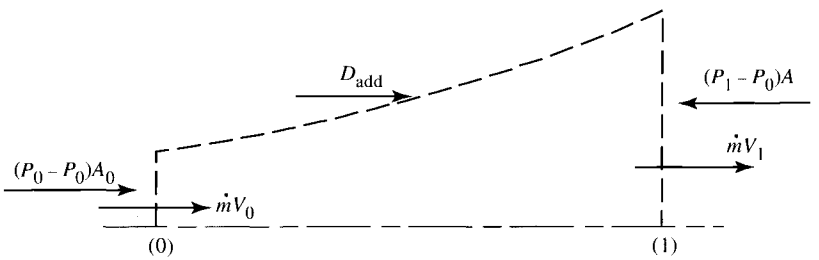

Fig. 4.4 Momentum equation applied to stream tube of engine air from 0 to 1.

The term $P + \rho V^2/g_c$ within the integrals is called the *total momentum flux*, and for a perfect gas

$$P + \frac{\rho V^2}{g_c} = P(1 + \gamma M^2) \tag{4.7}$$

Thus Eq. (4.6) can be expressed as

$$D_{\text{add}} = \int_1 P(1 + \gamma M^2)\mathrm{d}A_y - \int_0 \mathrm{P}(1 + \gamma M^2)\mathrm{d}A_y - P_0(A_1 - A_0)$$

For one-dimensional flow, this equation becomes

$$D_{\text{add}} = P_1A_1(1 + \gamma M_1^2) - P_0A_0(1 + \gamma M_0^2) - P_0(A_1 - A_0) \tag{4.8}$$

or

$$D_{\text{add}} = P_1A_1(1 + \gamma M_1^2) - P_0A_0\gamma M_0^2 - P_0A_1 \tag{4.9}$$

In the limit, as M_0 goes to zero, the $A_0M_0^2$ goes to zero, and Eq. (4.9) reduces to

$$(D_{\text{add}})_{M_0=0} = P_1A_1(1 + \gamma M_1^2) - P_0A_1 \tag{4.10}$$

Example 4.1

Two nacelles with inlet areas of (1) $A_1 = 0.20\,\text{m}^2$ and (2) $A_1 = 0.26\,\text{m}^2$ are being considered for use with a gas turbine engine X that produces an uninstalled thrust F of 20,000 N at sea level and $M_0 = 0.5$. Compare the installed engine thrust obtained with nacelle 1 and engine X to the installed engine thrust for nacalle 2 and engine X at $M_0 = 0.5$ and sea level. Engine X has a mass flow of 41.75 kg/s. Nacelles 1 and 2 each have the same nacelle drag of 900 N.

Solution: The installed engine thrust is given by

$$T = F - D = F - D_{\text{nac}} - D_{\text{add}}$$

Because both the uninstalled engine thrust F and nacelle drag D_{nac} are known, only the additive drag D_{add} need be determined for both nacelles. Either Eq. (4.8) or Eq. (4.9) can be used to calculate D_{add}, and both require the evaluation of P_1, M_1, and A_0. Because the mass flow rate into engine X is the same for both nacelles, A_0 will be determined first. The *mass flow parameter* (MFP) can

be used to find A_0 once the total temperature and pressure are known at station 0:

$$T_{t0} = T_0\left(1 + \frac{\gamma - 1}{2}M_0^2\right) = 288.2(1 + 0.2 \times 0.5^2) = 302.6\,\text{K}$$

$$P_{t0} = P_0\left(1 + \frac{\gamma - 1}{2}M_0^2\right)^{\gamma/(\gamma-1)} = 101{,}300(1 + 0.2 \times 0.5^2)^{35} = 120{,}160\,\text{Pa}$$

$$\text{MFP}(0.5)\sqrt{\frac{R}{g_c}} = \frac{\dot{m}\sqrt{T_{t0}}}{P_{t0}A_0}\sqrt{\frac{R}{g_c}} = 0.511053 \qquad \text{from Appendix E}$$

Thus

$$A_0 = \frac{\dot{m}\sqrt{T_{t0}}\sqrt{R/g_c}}{P_{t0}[\text{MFP}(0.5)\sqrt{R/g_c}]} = \frac{41.75\sqrt{302.6}(16.9115)}{120{,}160(0.511053)}$$
$$= 0.200\,\text{m}^2$$

With subsonic flow between stations 0 and 1, the flow between these two stations is assumed to be isentropic. Thus the total pressure and total temperature at station 1 are 120,160 Pa and 302.6 K. Because the mass flow rate, area, and total properties are known at station 1 for both nacelles, the Mach number M_1 and static pressure P_1 needed to calculate the additive drag can be determined as follows:

1) Calculate $\text{MFP}\sqrt{R/g_c}$ at station 1, and find M_1 from Appendix E.

2) Calculate P_1, using Eq. (3.10) or P/P_t from Appendix E.

Nacelle 1: Since the inlet area A_1 for nacelle 1 is the same as flow area A_0 and the flow process is isentropic, then $M_1 = 0.5$ and $P_1 = 101{,}300$ Pa. From Eq. (4.8), the additive drag is zero, and the installed thrust is

$$T = F - D_{\text{nac}} - D_{\text{add}} = 20{,}000 - 900 - 0 = 19{,}100\,\text{N}$$

Nacelle 2: Calculating $\text{MFP}\sqrt{R/g_c}$ at station 1, we find

$$\text{MFP}(M_1) = \frac{\dot{m}\sqrt{T_{t1}}}{P_{t1}A_1} = \frac{41.75\sqrt{302.6}}{120{,}160(0.26)}$$
$$= 0.0232465$$

From GASTAB, $M_1 = 0.3594$ and

$$P_1 = \frac{P_{t1}}{\{1 + [(\gamma - 1)/2]M_1^2\}^{\gamma/(\gamma-1)}} = \frac{120{,}160\,\text{Pa}}{1.09340} = 109.900\,\text{Pa}$$

Then, using Eq. (4.8), we have

$$\begin{aligned} D_{\text{add}} &= P_1A_1(1 + \gamma M_1^2) - P_0A_0(1 + \gamma M_0^2) - P_0(A_1 - A_0) \\ &= 109{,}900 \times 0.26(1 + 1.4 \times 0.3594^2) - 101{,}300 \\ &\quad \times 0.2(1 + 1.4 \times 0.5^2) - 101{,}300(0.26 - 0.20) \\ &= 33{,}741 - 27{,}351 - 6078 = 312\,\text{N} \\ T &= F - D_{\text{nac}} - D_{\text{add}} = 20{,}000 - 900 - 312 = 18{,}788\,\text{N} \end{aligned}$$

Conclusion: A comparison of the installed engine thrust T of nacelle 1 to that of nacelle 2 shows that nacelle 1 gives a higher installed engine thrust and is better than nacelle 2 at the conditions calculated.

Example 4.2

An inlet of about 48 ft^2 (a little larger than the inlet on one of the C5A's engines) is designed to have an inlet Mach number of 0.8 at sea level. Determine the variation of the additive drag with flight Mach number from $M_0 = 0$ to 0.9. Assume that M_1 remains constant at 0.8.

Solution: We will be using Eqs. (4.8) and (4.10) to solve this problem. The following values are known:

$$P_0 = 14.696\ \text{psia}, \quad M_1 = 0.8, \quad A_1 = 48\,\text{ft}^2, \quad \gamma = 1.4$$

Thus we must find values of A_0 and P_1 for each flight Mach number M_0. We assume isentropic flow between stations 0 and 1, and therefore P_t and A^* are constant. Using the relations for isentropic flow, We can write

$$P_1 = P_0 \frac{P_{t0}}{P_0} \frac{P_1}{P_{t1}} = P_0 \frac{(P/P_t)_1}{(P/P_t)_0}$$

$$A_0 = A_1 \frac{A_1^*}{A_1} \frac{A_0}{A_0^*} = A_1 \frac{(A/A^*)_0}{(A/A^*)_1}$$

We obtain values of P/P_t and A/A^* from the isentropic table (GASTAB program). At a flight Mach number of 0.9, we have

$$P_1 = P_0 \frac{(P/P_t)_1}{(P/P_t)_0} = 14.696\left(\frac{0.65602}{0.59126}\right) = 16.306\,\text{psia}$$

$$A_0 = A_1 \frac{(A/A^*)_0}{(A/A^*)_1} = 48\left(\frac{1.0089}{1.0382}\right) = 46.65\,\text{ft}^2$$

Table 4.1 Summary of additive calculations for Example 4.2

M_0	$\left(\frac{P}{P_t}\right)_0$	P_1, psia	$\left(\frac{A}{A^*}\right)_0$	A_0, ft^2	$1+\gamma M_0^2$	D_{add}, lbf
0.0	1.00000	9.641	—	—	1.000	24,768
0.1	0.99303	9.711	5.8218	269.16	1.014	17,711
0.2	0.97250	9.916	2.9635	137.01	1.056	12,135
0.3	0.93947	10.265	2.0351	94.09	1.126	7,857
0.4	0.89561	10.768	1.5901	73.52	1.224	4,687
0.5	0.84302	11.439	1.3398	61.94	1.350	2,453
0.6	0.78400	12.300	1.1882	54.94	1.504	1,017
0.7	0.72093	13.376	1.0944	50.60	1.686	258
0.8	0.65602	14.696	1.0382	48.00	1.896	0
0.9	0.59126	16.306	1.0089	46.65	2.134	164

Thus

$$\begin{aligned} D_{\text{add}} &= P_1A_1(1+\gamma M_1^2) - P_0A_0(1+\gamma M_0^2) - P_0(A_1 - A_0) \\ &= 16.306(144)(48)(1.896) - 14.696(144)(46.65)(2.134) \\ &\quad - 14.696(144)(1.35) \\ &= 213{,}693 - 210{,}672 - 2857 \\ &= 164 \text{ lbf} \end{aligned}$$

At a flight Mach number of 0, we have

$$(D_{\text{add}})_{M_0=0} = P_1A_1(1+\gamma M_1^2) - P_0A_1$$

$$P_t = (14.696)(0.65602) = 9.641 \text{ psia}$$

Thus

$$\begin{aligned} D_{\text{add}} &= 9.641(144)(48)(1.896) - 14.696(144)(48) \\ &= 126{,}347 - 101{,}579 \\ &= 24{,}768 \text{ lbf} \end{aligned}$$

Table 4.1 presents the results of this inlet's additive drag in the range of flight Mach numbers requested. As indicated in this table, the additive drag is largest at low flight Mach numbers for this fixed-area inlet.

As will be shown next, most of the additive drag D_{add} can be offset by the forebody portion of the nacelle drag (D_w, a negative drag or thrust), provided that the flow does not separate (in perfect flow, we will show that $D_{\text{add}} + D_w = 0$) with the large variation in M_0 and the fixed value of M_1,

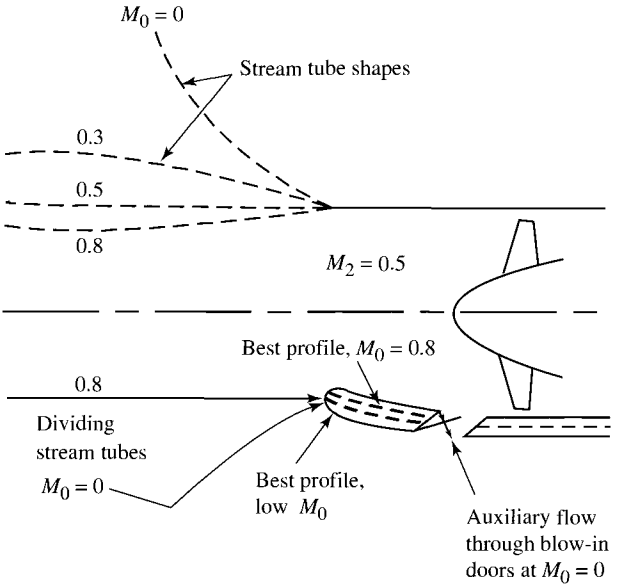

Fig. 4.5 Subsonic inlet at different flight Mach numbers (top) with auxiliary blow-in door (bottom) (from Ref. 28).

the path of the streamlines entering the inlet must go through large changes in geometry, as shown in Fig. 4.5. Boundary-layer separation on the forebody of the nacelle can occur when the inlet must turn the flow through large angles with a resulting decrease in the magnitude of the drag on the forebody portion of the nacelle and increase in the net drag $D_{\text{add}} + D_w$ on the front portion of the inlet. To reduce the additive drag at low flight Mach numbers, some subsonic inlets have blow-in doors or auxiliary inlets (see Fig. 4.5) that increase the inlet area at the low flight Mach numbers (full-throttle operation) and thus reduce the additive drag.

In the relationship between nacelle drag and additive drag, the nacelle drag and the additive drag are interdependent. We can learn something about this interdependence by considering a *perfect nacelle*, i.e., a nacelle with no external viscous drag or form drag.

We now consider a control volume for all of the fluid flowing external to the engine, i.e., all of the fluid outside the stream tube shown in Fig. 4.6. Because the flow is perfect (no shocks, no boundary layers, etc.), the fluid conditions are identical at the entrance 0 and exit 9 of our control volume.

Because the momentum of the fluid flowing through the control volume does not change, the sum of the pressure forces acting on the inside of the stream tube must equal zero. For perfect flow, we have

$$\int_0^1 (P - P_0)\mathrm{d}A_y + \int_1^9 (P - P_0)\mathrm{d}A_y + \int_9^\infty (P - P_0)\mathrm{d}A_y = 0$$

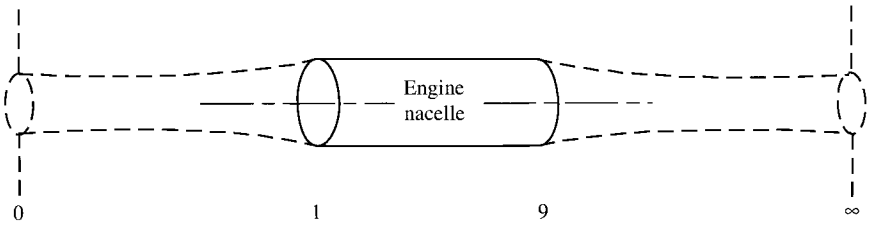

Fig. 4.6 Stream tube of flow through engine nacelle.

or

$$D_{\text{add}} + D_{\text{nac}} = -\int_{9}^{\infty} (P - P_0)\mathrm{d}A_y \tag{4.11}$$

For the case of a perfect fluid, we can combine Eqs. (4.11), (4.6), (4.3), and (4.2) to obtain

$$T = F + \int_{9}^{\infty} (P - P_0)\mathrm{d}A_y \tag{4.12}$$

For a perfectly expanded nozzle ($P_9 = P_0$) and a jet that is parallel to the free-stream ($\mathrm{d}A_y = 0$), the following conclusions can be made:

1) From Eq. (4.11), the sum of the additive drag and nacelle drag is zero.
2) From Eq. (4.12), the installed engine thrust T equals the uninstalled engine thrust F.

It is industry practice to break the nacelle drag into two components: the drag associated with the forebody (front half of nacelle) D_w and the drag associated with the afterbody (rear half of nacelle) D_b. This is usually a reasonable approach because often lip separation dominates near the inlet and boat-tail drag near the exit. Assuming the division of nacelle drag to be meaningful, we can interpret the two drag terms by considering the nacelle to be very long and parallel in the middle, as shown in Fig. 4.7.

In this case, perfect flow would give us P_0, etc., at the middle. Application of the momentum equation to a control volume from 0 to m containing all of the

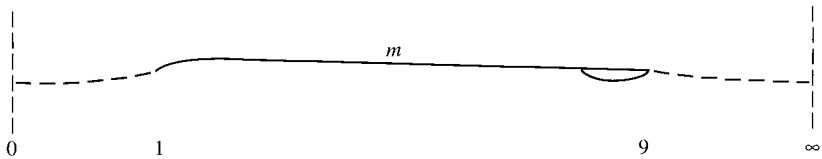

Fig. 4.7 Ideal long nacelle.

fluid outside the engine's stream tube will give

$$\int_0^1 (P - P_0)\mathrm{d}A_y + \int_1^m (P - P_0)\mathrm{d}A_y = 0$$

That is, in perfect flow,

$$D_{\text{add}} + D_{\text{w}} = 0 \tag{4.13}$$

similarly, application of the momentum equation to a control from m to ∞ containing all of the fluid outside the engine's stream tube will give

$$D_b + \int_9^\infty (P - P_0)\mathrm{d}A_y = 0 \tag{4.14}$$

4.3 Note on Propulsive Efficiency

The kinetic energy of the fluid flowing through an aircraft propulsion system is increased by an energy-transfer mechanism consisting of a series of processes constituting an engine cycle. From the point of view of an observer riding on the propulsion unit (see Fig. 4.8a), the engine cycle output is the increase of kinetic energy received by the air passing through the engine, which is $(V_9^2 - V_0^2)/(2g_c)$. From this observer's point of view, the total power output of the engine is the kinetic energy increase imparted to the air per unit time. On the other hand, from the point of view of an observer on the ground (see Fig. 4.8b), one sees the aircraft propulsion system's thrust moving at a velocity V_0 and observes the still air to receive an increase in kinetic energy, after passing through the engine, by an amount $(V_9 - V_0)^2/(2g_c)$. From this point of view, therefore, the total effect of the engine (and its output) is the sum of the propulsive power FV_0 and the kinetic energy per unit time imparted to the air passing through the engine. The sole purpose of the engine is to produce a propulsive power, and this is called the *useful power output* of the propulsion system. The ratio of the useful power output to the total power output of the propulsion system is called the *propulsive efficiency* [see Eq. (1.14)].

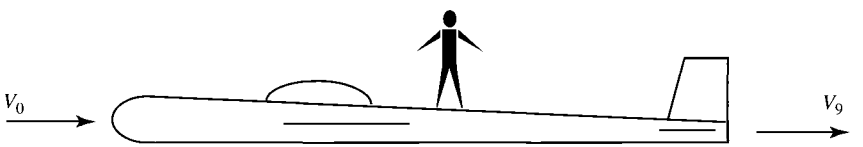

Fig. 4.8a Velocity change by observer on aircraft.

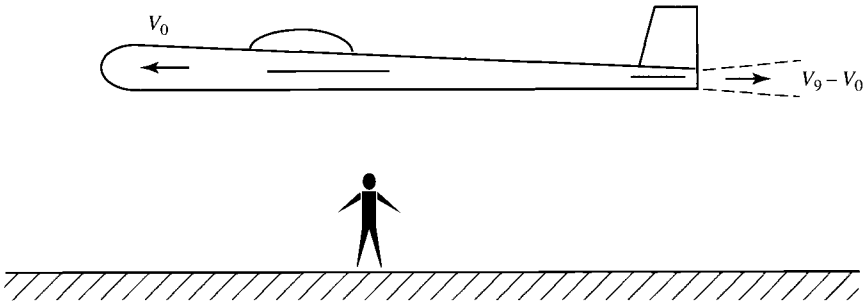

Fig. 4.8b Velocity change by observer on ground.

4.4 Gas Turbine Engine Components

The inlet, compressor, combustor, turbine, and nozzle are the main components of the gas turbine engine. The purpose and operation of these components and two thrust augmentation techniques are discussed in this section.

4.4.1 Inlets

An inlet reduces the entering air velocity to a level suitable for the compressor. The air velocity is reduced by a compression process that increases the air pressure. The operation and design of the inlet are described in terms of the efficiency of the compression process, the external drag of the inlet, and the mass flow into the inlet. The design and operation of the inlet depend on whether the air entering the duct is subsonic or supersonic. As the aircraft approaches the speed of sound, the air tends to be compressed more, and at Mach 1, shock waves occur. Shock waves are compression waves, and at higher Mach numbers, these compression waves are stronger. Compression by shock waves is inefficient. In subsonic flow, there are no shock waves, and the air compression takes place quite efficiently. In supersonic flow, there are shock waves present. Shock waves and the compressibility of air then influence the design of inlets.

4.4.1.1 Subsonic inlet. The subsonic inlet can be a divergent duct, as shown in Fig. 4.9. This duct is satisfactory until the Match number becomes greater than 1, at which time a shock wave occurs at the mouth and the compression process becomes inefficient. The subsonic divergent duct operates

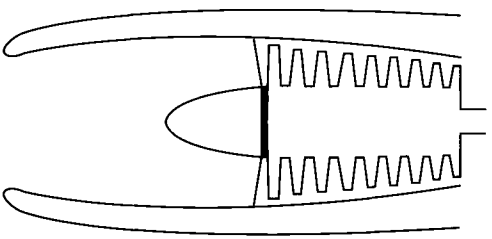

Fig. 4.9 Subsonic inlet.

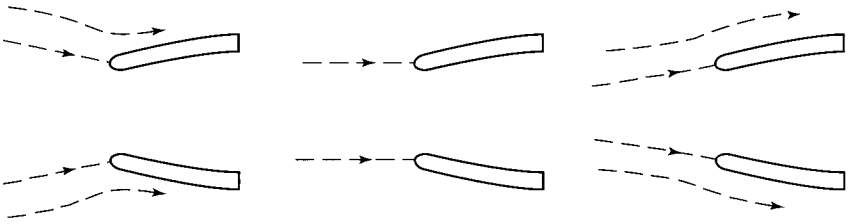

Fig. 4.10 Subsonic inlet flow patterns.

best at one velocity (design point), and at other velocities, the compression process is less efficient and the external drag is greater. The airflow patterns for the subsonic inlet are shown in Fig. 4.10.

4.4.1.2 Supersonic inlet. Because shock waves will occur in supersonic flow, the geometry of supersonic inlets is designed to obtain the most efficient compression with a minimum of weight. If the velocity is reduced from a supersonic speed to a subsonic speed with one normal shock wave, the compression process is relatively inefficient. If several oblique shock waves are employed to reduce the velocity, the compression process is more efficient. Two typical supersonic inlets are the *ramp* (two-dimensional wedge) and the *centerbody* (three-dimensional spike), which are shown in Fig. 4.11. The shock wave positions in Fig. 4.11 are for the design condition of the inlet. At off-design Mach numbers, the positions of the shock waves change, thus affecting the external drag and the efficiency of compression. A more efficient ramp or centerbody inlet can be designed by using more than two shock waves to compress the entering air. Also, if the geometry is designed to be variable, the inlet operates more efficiently over a range of Mach numbers.

4.4.2 Compressors

The function of the compressor is to increase the pressure of the incoming air so that the combustion process and the power extraction process after combustion can be carried out more efficiently. By increasing the pressure of the air, the volume of the air is reduced, which means that the combustion of the fuel/air mixture will occur in a smaller volume.

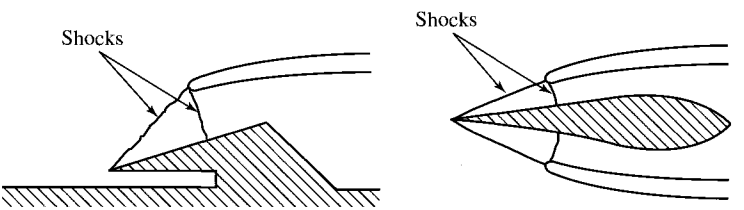

Fig. 4.11 Supersonic inlets.

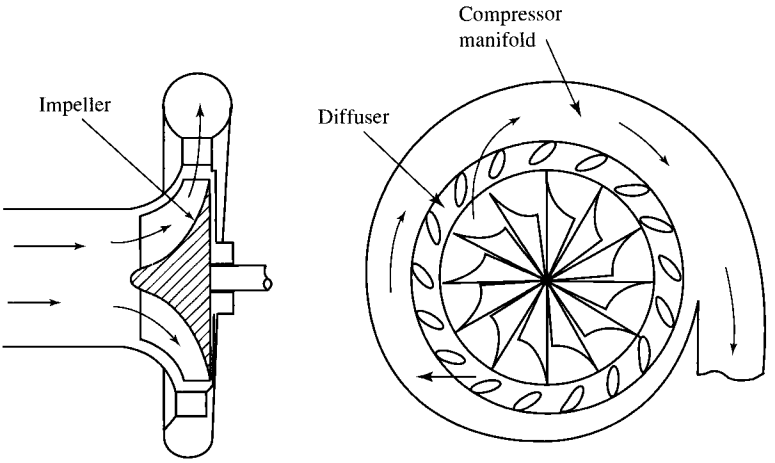

Fig. 4.12 Single-stage centrifugal compressor.

4.4.2.1 Centrifugal compressor. The compressor was the main stumbling block during the early years of turbojet engine development. Great Britain's Sir Frank Whittle solved the problem by using a centrifugal compressor. This type of compressor is still being used in many of the smaller gas turbine engines. A typical single-stage centrifugal compressor is shown in Fig. 4.12. The compressor consists of three main parts: an impeller, a diffuser, and a compressor manifold. Air enters the compressor near the hub of the impeller and is then compressed by the rotational motion of the impeller. The compression occurs by first increasing the velocity of the air (through rotation) and then diffusing the air where the velocity decreases and the pressure increases. The diffuser also straightens the flow, and the manifold serves as a collector to feed the air into the combustor. The single-stage centrifugal compressor has a low efficiency and a maximum compression ratio of 4:1 or 5:1. Multistage centrifugal compressors are somewhat better, but an axial compressor offers more advantages.

4.4.2.2 Axial compressors. An axial compressor is shown in Fig. 4.13. The air in an axial compressor flows in an axial direction through a series of rotating *rotor* blades and stationary *stator* vanes that are concentric with the axis of rotation. Each set of rotor blades and stator vanes is known as a *stage*. The flow

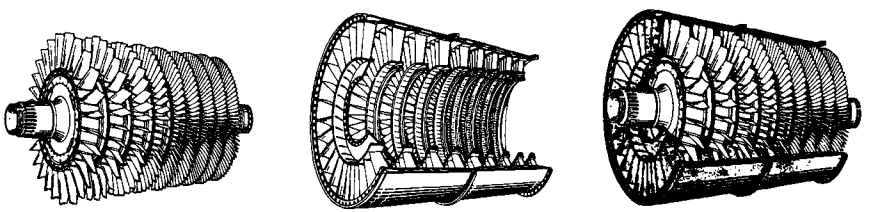

Fig. 4.13 Multistage axial compressor. (Courtesy of Pratt & Whitney.)

path in an axial compressor decreases in the cross-sectional area in the direction of flow. The decrease of area is in proportion to the increased density of the air as the compression progresses from stage to stage. Figure 4.13 contains a schematic of an axial compressor. Each stage of an axial compressor produces a small compression pressure ratio (1.1:1 to 1.2:1) at a high efficiency. Therefore, for high pressure ratios (12:1), multiple stages are used. Axial compressors are also more compact and have a smaller frontal area than a centrifugal compressor, which are added advantages. For the best axial compressor efficiency, the compressor operates at a constant axial velocity, as shown in Fig. 1.6. At high compression ratios, multistaging a single axial compressor does not produce as efficient an operation as a dual axial compressor would (see Fig. 1.4a). For a single rotational speed, there is a limit in the balance operation between the first and last stages of the compressor. To obtain more flexibility and a more uniform loading of each compressor stage, a dual compressor with two different rotational speeds is generally used in high-compression-ratio axial compressors.

4.4.3 Combustor or Main Burner

The combustor is designed to burn a mixture of fuel and air and to deliver the resulting gases to the turbine at a uniform temperature. The gas temperature must not exceed the allowable structural temperature of the turbine. A schematic of a combustor is shown in Fig. 4.14. About one-half of the total volume of air entering the burner mixes with the fuel and burns. The rest of the air—secondary air—is simply heated or may be thought of as cooling the products of combustion and cooling the burner surfaces. The ratio of total air to fuel varies among the different types of engines from 30 to 60 parts of air to 1 part of fuel by weight. The average ratio in new engine designs is about 40:1, but only 15 parts are used for burning (since the combustion process demands that the number of parts of air to fuel must be within certain limits at a given pressure for combustion to occur). Combustion chambers may be of the can, the annular, or the can-annular type, as shown in Fig. 4.15.

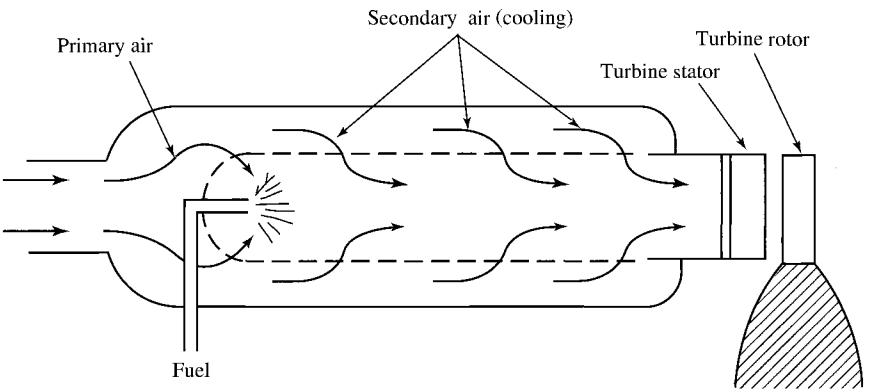

Fig. 4.14 Straight-through flow combustor.

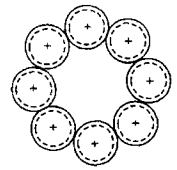

a) Can

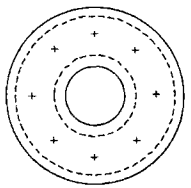

b) Annular

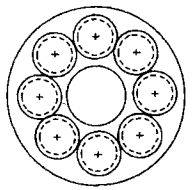

c) Can annular

Casing

Liner

Fuel inlet

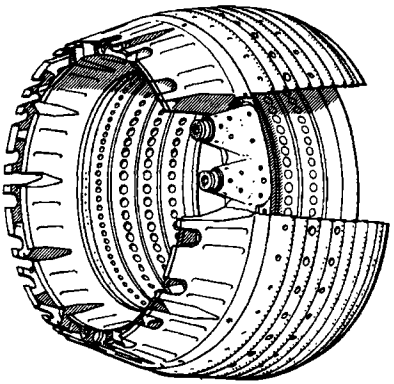

Typical annular-type combustion chamber

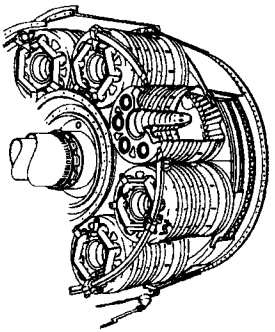

Typical can-annular-type combustion chamber

Fig. 4.15 Cross sections of combustion chambers. (Courtesy of Pratt & Whitney.)

For an acceptable burner design, the pressure loss as the gases pass through the burner must be held to a minimum, the combustion efficiency must be high, and there must be no tendency for the burner to blow out (flameout). Also, combustion must take place entirely within the burner.

4.4.4 Turbines

The turbine extracts kinetic energy from the expanding gases that flow from the combustion chamber. The kinetic energy is converted to shaft horsepower to drive the compressor and the accessories. Nearly three-fourths of all the energy available from the products of combustion is required to drive the compressor. The axial-flow turbine consists of a turbine wheel *rotor* and a set of stationary vanes *stator*, as shown in Fig. 4.16. The set of stationary vanes of the turbine is a plane of vanes (concentric with the axis of the turbine) that are set at an angle to form a series of small nozzles that discharge the gases onto the blades of the turbine wheel. The discharge of the gases onto the rotor

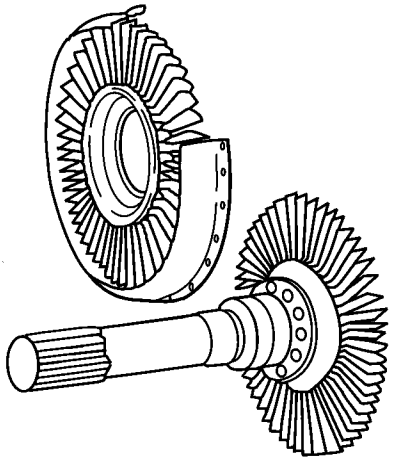

Fig. 4.16 Axial-flow turbine components.

allows the kinetic energy of the gases to be transformed to mechanical shaft energy.

Like the axial compressor, the axial turbine is usually multistaged. There are generally fewer turbine stages than compressor stages because in the turbine the pressure is decreasing (expansion process), whereas in the compressor the pressure is increasing (compression process). In each process (expansion or compression), the blades of the axial turbine or axial compressor act as airfoils, and the airflow over the airfoil is more favorable in the expansion process. The result is that one stage of turbine can power many compressor stages.

4.4.4.1 Impulse turbine. The impulse turbine and the reaction turbine are the two basic types of axial turbines, as shown in Fig. 4.17. In the impulse type, the relative discharge velocity of the rotor is the same as the relative inlet velocity because there is no net change in pressure between the rotor inlet and rotor exit. The stator nozzles of the impulse turbine are shaped to form passages that increase the velocity and reduce the pressure of the escaping gases.

4.4.4.2 Reaction turbine. In the reaction turbine, the relative discharge velocity of the rotor increases and the pressure decreases in the passages between rotor blades. The stator nozzle passages of the reaction turbine merely alter the direction of the flow.

Most turbines in jet engines are a combination of impulse and reaction turbines. In the design of turbines, the following items must be considered: 1) shaft rotational speed, 2) gas flow rate, 3) inlet and outlet temperatures, 4) inlet and outlet pressures, 5) exhaust velocity, and 6) required power output. If the jet engine is equipped with a dual compressor, the turbine must also be dual or split.

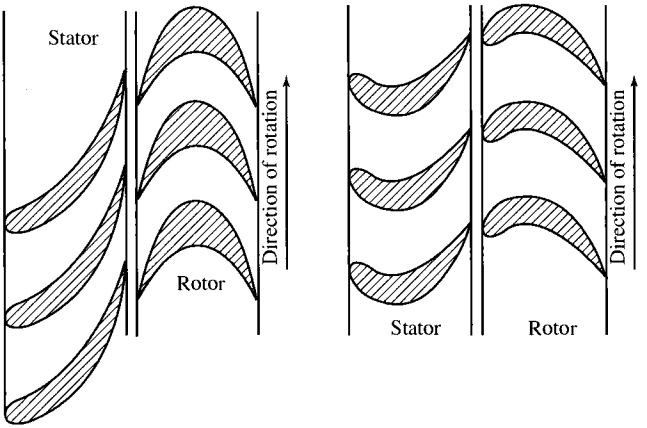

a) Impulse **b) Reaction**

Fig. 4.17 Impulse and reaction stages.

4.4.5 Exhaust Nozzle

The purpose of the exhaust nozzle is to increase the velocity of the exhaust gas before discharge from the nozzle and to collect and straighten gas flow from the turbine. In operating, the gas turbine engine converts the internal energy of the fuel to kinetic energy in the exhaust gas stream. The net thrust (or force) of the engine is the result of this operation, and it can be calculated by applying Newton's second law of motion (see Chapter 2). For large values of specific thrust, the kinetic energy of the exhaust gas must be high, which implies a high exhaust velocity. The nozzle supplies a high exit velocity by expanding the exhaust gas in an expansion process that requires a decrease in pressure. The pressure ratio across the nozzle controls the expansion process, and the maximum thrust for a given engine is obtained when the exit pressure equals the ambient pressure. Nozzles and their operation are discussed further in Chapters 2, 3, and 10. The two basic types of nozzles used in jet engines are the convergent and convergent-divergent nozzles.

4.4.5.1 Convergent nozzle. The convergent nozzle is a simple convergent duct, as shown in Fig. 4.18. When the nozzle pressure ratio (turbine exit pressure to nozzle exit pressure) is low (less than about 2), the convergent nozzle is used. The convergent nozzle has generally been used in low-thrust engines for subsonic aircraft.

4.4.5.2 Convergent-divergent nozzle. The convergent-divergent nozzle can be a convergent duct followed by a divergent duct. Where the cross-sectional area of the duct is a minimum, the nozzle is said to have a *throat* at that position. Most convergent-divergent nozzles used in supersonic aircraft are not simple

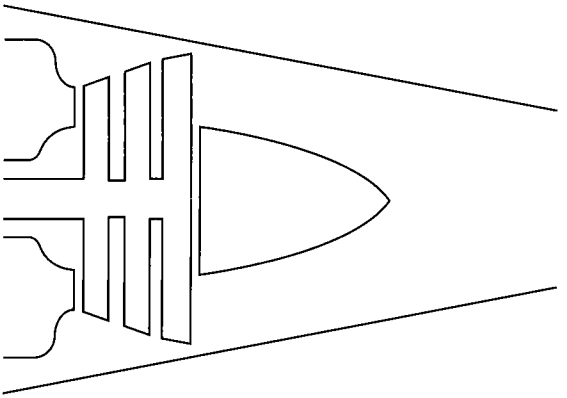

Fig. 4.18 Convergent exhaust nozzle.

ducts, but incorporate variable geometry and other aerodynamic features, as shown in Fig. 4.19. Only the throat area and exit area of the nozzle in Fig. 4.19 are set mechanically, the nozzle walls being determined aerodynamically by the gas flow. The convergent-divergent nozzle is used if the nozzle pressure ratio is high. High-specific-thrust engines in supersonic aircraft generally have some form of convergent-divergent nozzle. If the engine incorporates an afterburner, the nozzle throat and exit area must be varied to match the different flow conditions and to produce the maximum available thrust.

4.4.6 Thrust Augmentation

Thrust augmentation can be accomplished by either water injection or afterburning.

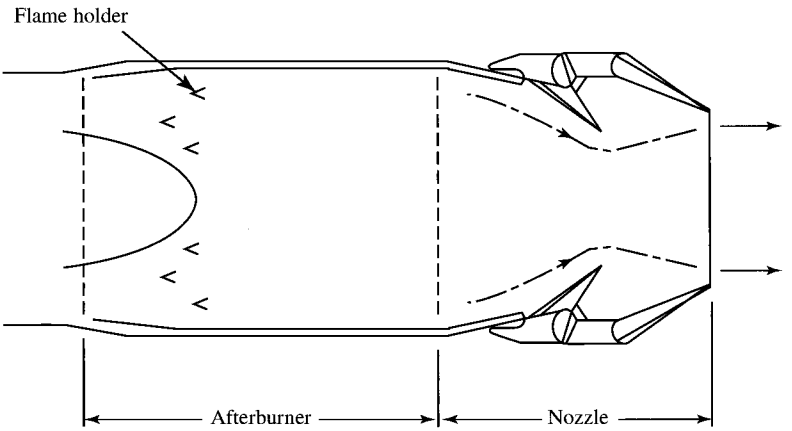

Fig. 4.19 Convergent-divergent ejector exhaust nozzle. (Courtesy of Pratt & Whitney.)

4.4.6.1 Water injection. Thrust augmentation by water injection (or by water/alcohol mixture) is achieved by injecting water into either the compressor or the combustion chamber. When water is injected into the inlet of the compressor, the mass flow rate increases and a higher combustion chamber pressure results if the turbine can handle the increased mass flow rate. The higher pressure and the increase in mass flow combine to increase the thrust. Injection of water into the combustion chamber produces the same effect, but to a lesser degree and with greater consumption of water. Water injection on a hot day can increase the takeoff thrust by as much as 50% because the original mass of air entering the jet engine is less for a hot day. The amount of air entering any turbomachine is determined by its volumetric constraints; therefore, it follows that the mass flow on a hot day will be less because the air is less dense on a hot day.

4.4.6.2 Afterburning. Another method of thrust augmentation is by burning additional fuel in the afterburner. The afterburner is a section of duct between the turbine and exhaust nozzle. The schematic diagram in Fig. 4.19 shows the afterburner section. The afterburner consists of the duct section, fuel injectors, and flame holders. It is possible to have afterburning because, in the main burner section, the combustion products are air-rich. The effect of the afterburning operation is to raise the temperature of the exhaust gases that, when exhausted through the nozzle, will reach a higher exit velocity. The pressure/temperature velocity profile for afterburning is also shown in Fig 1.6. The J79 for afterburner operation has a thrust of 17,900 lbf and a *thrust specific fuel consumption* (TSFC) of 1.965 [(lbm/h)/lbf]/h, and for military operation (no afterburning) it has a thrust of 11,870 lbf and a TSFC of 0.84 [(lbm/h)/lbf]/h. We then see that afterburning produces large thrust gains at the expense of fuel economy.

4.5 Brayton Cycle

The Brayton power cycle is a model used in thermodynamics for an ideal gas turbine power cycle. It is composed of the four following processes, which are also shown in Fig. 4.20a:

1) Isentropic compression (2 to 3)
2) Constant-pressure heat addition (3 to 4)
3) Isentropic expansion (4 to 9)
4) Constant-pressure heat rejection (9 to 2)

The basic components of the Brayton cycle are shown to the right in Fig. 4.20b. In the ideal cycle, the processes through both the compressor and the turbine are considered to be reversible and adiabatic (isentropic). The processes through the heater and cooler are considered to be constant-pressure in the ideal cycle.

For a calorically perfect gas, thermodynamic analysis of the ideal Brayton cycle gives the following equations for the rate of energy transfer of each

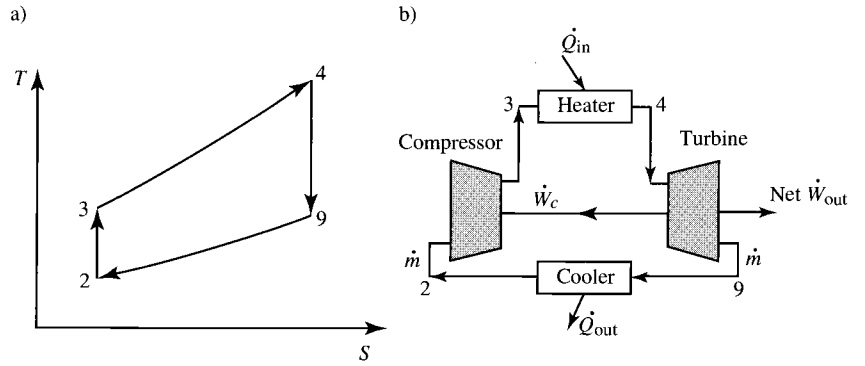

Fig. 4.20 Brayton cycle.

component:

$$\dot{W}_c = \dot{m}c_p(T_3 - T_2) \qquad \dot{Q}_{in} = \dot{m}c_p(T_4 - T_3)$$
$$\dot{W}_t = \dot{m}c_p(T_4 - T_9) \qquad \dot{Q}_{out} = \dot{m}c_p(T_9 - T_2)$$
$$\text{Net } \dot{W}_{out} = \dot{W}_t - \dot{W}_c = \dot{m}c_p[T_4 - T_9 - (T_3 - T_2)]$$

Now, the thermal efficiency of the cycle is $\eta_T = \text{net } \dot{W}_{out}/\dot{Q}_{in}$. Noting that $(P_3/P_2)^{(\gamma-1)/\gamma} = T_3/T_2 = T_4/T_9$, we see that the thermal efficiency for the ideal Brayton cycle can be shown to be given by

$$\eta_T = 1 - \left(\frac{1}{\text{PR}}\right)^{(\gamma-1)/\gamma} \tag{4.15}$$

where PR is the *pressure ratio* P_3/P_2. The thermal efficiency is plotted in Fig. 4.21 as a function of the compressor pressure ratio for two ratios of specific heats.

For an ideal Brayton cycle with fixed compressor inlet temperature T_2 and heater exit temperature T_4, simple calculus yields an expression for the pressure ratio P_3/P_2 and associated temperature ratio T_3/T_2 giving the maximum net work output per unit mass. This optimum compressor pressure, or temperature ratio, corresponds to the maximum area within the cycle on a *T-s* diagram, as shown in Fig. 4.22. One can show that the optimum compressor temperature ratio is given by

$$\left(\frac{T_3}{T_2}\right)_{\text{max work}} = \sqrt{\frac{T_4}{T_2}} \tag{4.16}$$

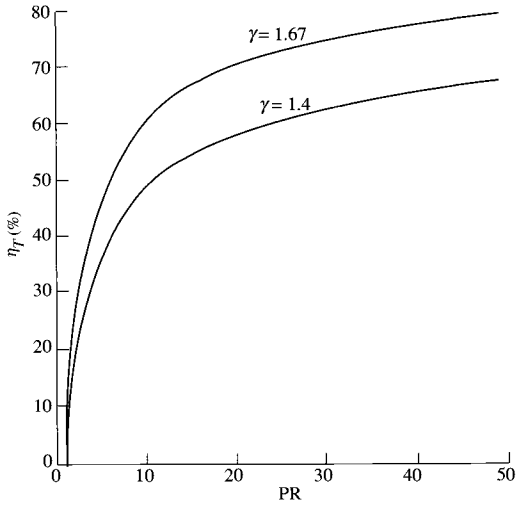

Fig. 4.21 Thermal efficiency of ideal Brayton cycle.

and the corresponding net work output per unit mass is given by

$$\frac{\text{Net } \dot{W}_{\text{out}}}{\dot{m}} = c_p T_2 \left(\sqrt{\frac{T_4}{T_2}} - 1 \right)^2 \tag{4.17}$$

which is plotted in Fig. 4.23 vs T_4 for air with $T_2 = 288$ K.

Three variations in the basic Brayton cycle are shown in Figs. 4.24–4.26. Figure 4.24 shows the cycle with a *high-pressure* (HP) turbine driving the compressor and a free-power turbine providing the output power. This cycle has the same thermal efficiency as the ideal Brayton cycle of Fig. 4.20. Figure 4.25 shows the Brayton cycle with reheat. Addition of reheat to the cycle increases the specific power of the free turbine and reduces the thermal efficiency.

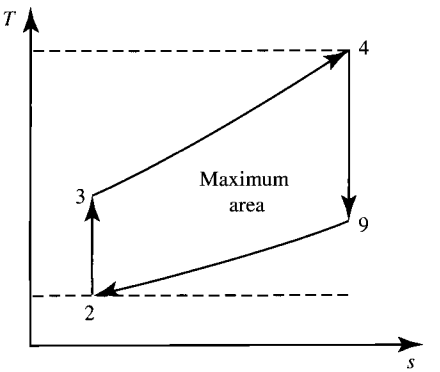

Fig. 4.22 Maxium-power-output Brayton cycle.

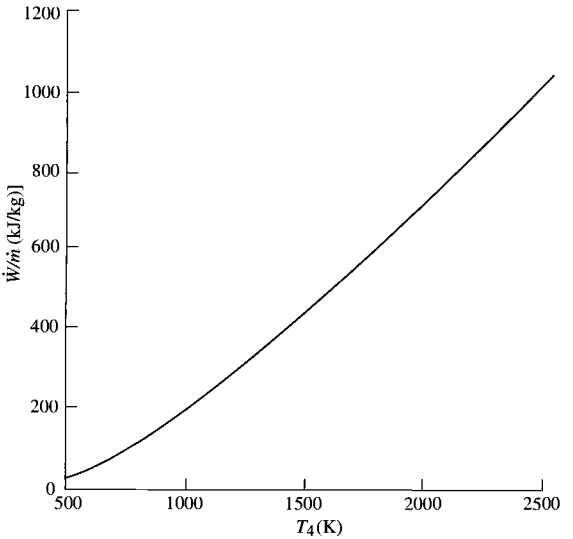

Fig. 4.23 Variation of maximum output power with T_4 for ideal Brayton cycle (T_2 = 288 K).

Figure 4.26 shows the ideal Brayton cycle with regeneration. When regeneration is added to the basic Brayton cycle, the energy input to the heater is reduced, which increases the cycle's thermal efficiency. For an ideal regenerator, we have

$$T_{3.5} = T_9 \qquad \text{and} \qquad T_{9.5} = T_3$$

Note that regeneration is possible only when T_9 is greater than T_3, which requires low cycle pressure ratios. The thermal efficiency of an ideal Brayton cycle with regeneration is shown in Fig. 4.27 for several values of T_4/T_2 along with the

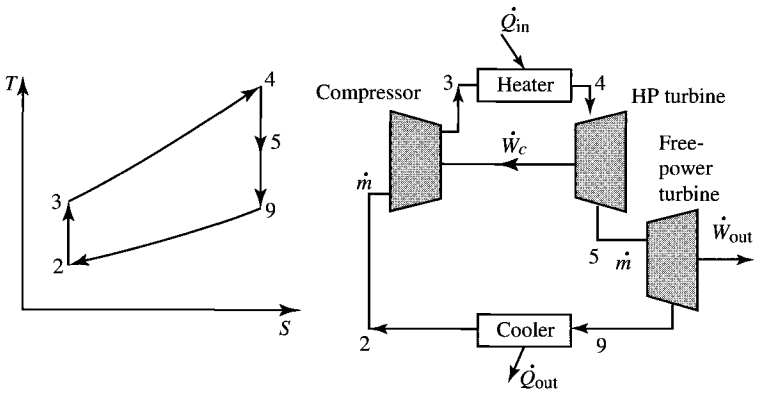

Fig. 4.24 Brayton cycle with free-power turbine.

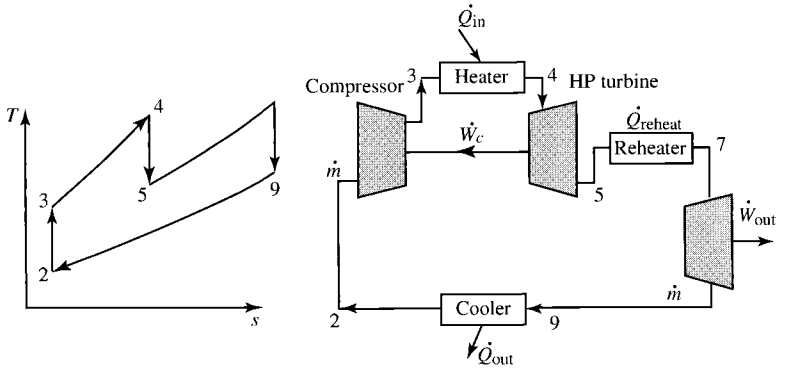

Fig. 4.25 Brayton cycle with reheat.

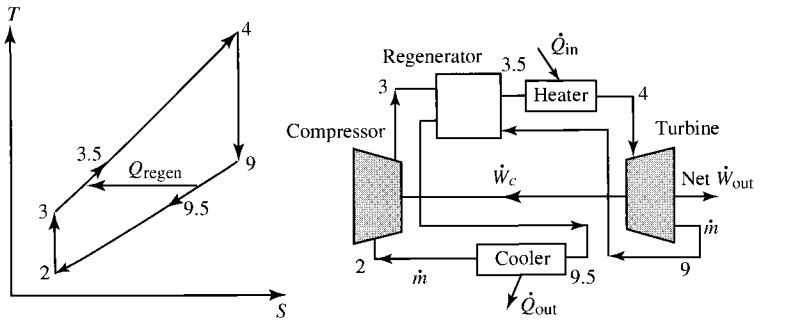

Fig. 4.26 Ideal Brayton cycle with regeneration.

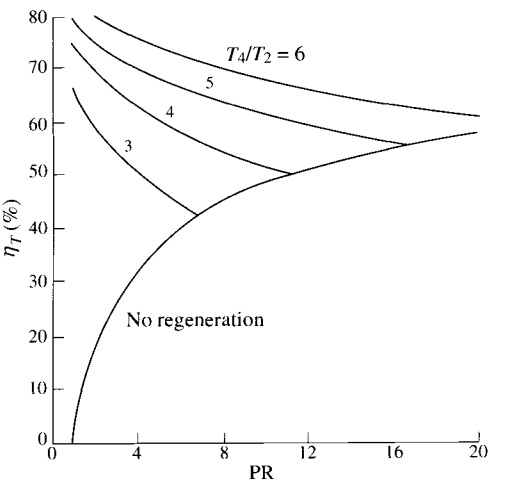

Fig. 4.27 Thermal efficiency of ideal Brayton cycle with regeneration.

thermal efficiency of the cycle without regeneration. The thermal efficiency of the ideal Brayton cycle with regeneration is given by

$$\eta_T = 1 - \frac{(\mathrm{PR})^{(\gamma-1)/\gamma}}{T_4/T_2} \tag{4.18}$$

4.6 Aircraft Engine Design

This introductory chapter to aircraft propulsion systems has presented the basic engine components and ideal engines. The following chapters present the cycle analysis (thermodynamic design-point study) of ideal and real engines, off-design performance, and an introduction to the aerodynamics of engine components. The design procedure for a typical gas turbine engine, shown in Fig. 4.28, requires that thermodynamic design-point studies (cycle analysis)

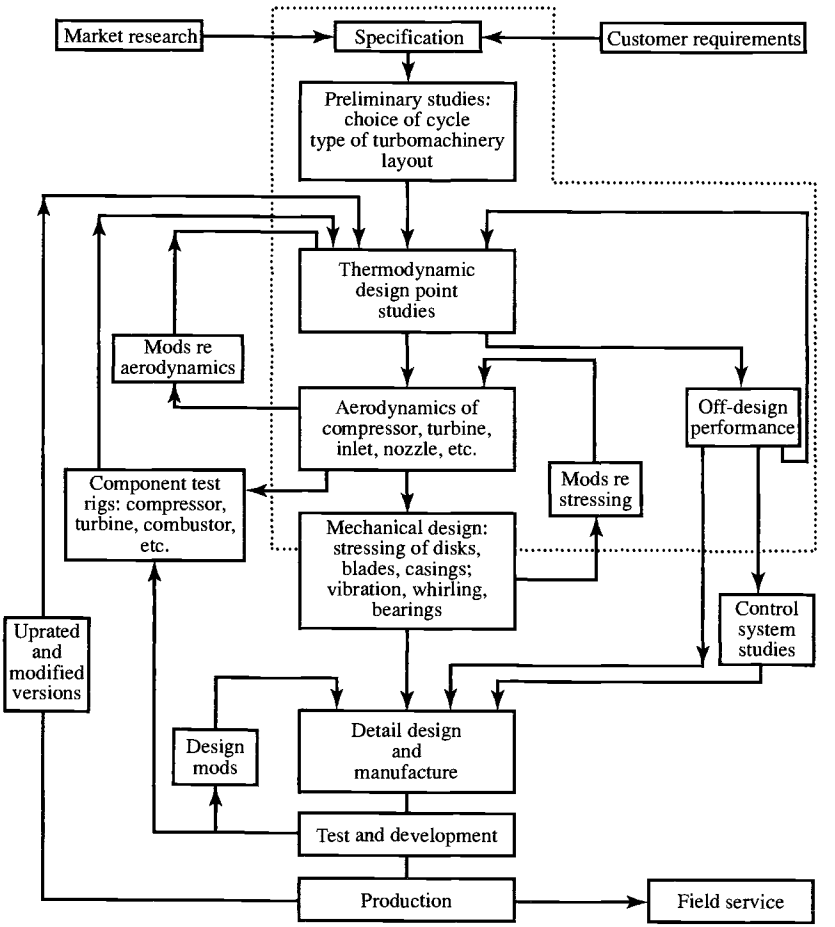

Fig. 4.28 Typical aircraft gas turbine design procedure (from Ref. 29).

and off-design performance be in the initial steps of design. The iterative nature of design is indicated in Fig. 4.28 by the feedback loops. Although only a few loops are shown, many more exist. Those items within the dashed lines of Fig. 4.28 are addressed within this textbook.

Problems

4.1 The inlet for a high-bypass-ratio turbofan engine has an area A_1 of 6.0 m^2 and is designed to have an inlet Mach number M_1 of 0.6. Determine the additive drag at the flight conditions of sea-level static test and Mach number of 0.8 at 12-km altitude.

4.2 An inlet with an area A_1 of 10 ft^2 is designed to have an inlet Mach number M_1 of 0.6. Determine the additive drag at the flight conditions of sea-level static test and Mach number of 0.8 at 40-kft altitude.

4.3 Determine the additive drag for an inlet having an area A_1 of 7000 $in.^2$ and a Mach number M_1 of 0.8 while flying at a Mach number M_0 of 0.4 at an altitude of 2000 ft.

4.4 Determine the additive drag for an inlet having an area A_1 of 5.0 m^2 and a Mach number M_1 of 0.7 while flying at a Mach number M_0 of 0.3 at an altitude of 1 km.

4.5 A turbojet engine under static test ($M_0 = 0$) has air with a mass flow of 100 kg/s flowing through an inlet area A_1 of 0.56 m^2 with a total pressure of 1 atm and total temperature of 288.8 K. Determine the additive drag of the inlet.

4.6 In Chapter 1, the loss in thrust due to the inlet is defined by Eq. (1.8) as $\phi_{\text{inlet}} = D_{\text{inlet}}/F$. Determine ϕ_{inlet} for the inlets of Example 4.1.

4.7 Determine the variation of inlet mass flow rate with Mach number M_0 for the inlet of Example 4.2

4.8 In Chapter 1, the loss in thrust due to the inlet is defined by Eq. (1.8) as $\phi_{\text{inlet}} = D_{\text{inlet}}/F$. For subsonic flight conditions, the additive drag D_{add} is a conservative estimate of D_{inlet}.

(a) Using Eq. (4.9) and isentropic flow relations, show that ϕ_{inlet} can be written as

$$\phi_{\text{inlet}} = \frac{D_{\text{add}}}{F} = \frac{(M_0/M_1)\sqrt{T_1/T_0}(1 + \gamma M_1^2) - (A_1/A_0 + \gamma M_0^2)}{(Fg_c/\dot{m}_0)(\gamma M_0/a_0)}$$

(b) Calculate and plot the variation of ϕ_{inlet} with flight Mach number M_0 from 0.2 to 0.9 for inlet Mach numbers M_1 of 0.6 and 0.8 with $(Fg_c/\dot{m}_0)(\gamma/a_0) = 4.5$.

4.9 A bell-mouth inlet (see Fig. P2.8) is installed for static testing of jet engines. Determine the force on the bell-mouth inlet with the data of Problem 2.34b for an inlet area that is 8 times the area at station 2 (assume that the inlet wall is a stream tube and that the outside of the bell-mouth inlet sees a static pressure equal to P_0.

4.10 The maximum power out of an ideal Brayton cycle operating between temperatures T_2 and T_4 is given by Eq. (4.17). By taking the derivative of the net work out of an ideal Brayton cycle with respect to the pressure ratio (PR) and setting it equal to zero, show that Eq. (4.16) gives the resulting compressor temperature ratio and Eq. (4.17) gives the net work out.

4.11 Show that Eq. (4.18) gives the thermal efficiency for the ideal Brayton cycle with regeneration.

4.12 For the ideal Brayton cycle with regeneration, regeneration is desirable when $T_9 \geq T_3$. Show that the maximum compressor pressure ratio $\mathrm{PR}_{\max}$ for regeneration ($T_9 = T_3$) is given by

$$\mathrm{PR}_{\max} = \left(\frac{T_4}{T_2}\right)^{\gamma/[2(\gamma-1)]}$$